Spectrum Sensing for Cognitive Radio Architectures based on sub-Nyquist Sampling Schemes

Volker Pohl*, Fiky Y. Suratman†, Abdelhak M. Zoubir†, Holger Boche*
* Institute for Theoretical Information Technology, TU München, Germany, {volker.pohl, boche}@tum.de
† Signal Process. Group, Inst. of Telecommunications., TU Darmstadt, Germany, {fsurat, zoubir}@spg.tu-darmstadt.de

***Abstract*—This paper investigates a signal processing architecture for cognitive radio based on a sub-Nyquist sampling of the wideband signal. Then spectrum scanning is performed by applying an adaptive digital filter to scan the bands which might be used for cognitive radio. In particular, the paper studies detectors which are tailored for the applied signal processing scheme and which takes into account the noise correlation, introduced by the digital scanning filter.**

***Index Terms*—Cognitive Radio, correlated noise, sub-Nyquist sampling.**

I. Introduction

In recent years, there has been increasing interest of consumers in wireless services, which has led to the evolution of wireless networks toward high-speed data networks. With many new introduced wireless services and the increasing need for mobile Internet access, demand for frequency band or spectrum is expected to grow continuously in years to come. However, with most of the spectrum being already allocated, it is hard to find vacant bands to either deploy new services or to enhance existing ones. Measurements have shown that most of the allocated spectrum is generally under-utilized. This is where cognitive radio technology comes into play with its inherent capability of spectrum opportunity detection or spectrum sensing [1], [2].

The idea of cognitive radio (CR) is to allow unlicensed or secondary users to use spectrum holes, which are the spectrum bands that are not being occupied by licensed or primary users. In order to detect spectrum holes, every secondary user should be equipped with spectrum sensing capability to monitor continuously the spectrum activities of licensed users in order to find a suitable spectrum band for possible utilization. Once the operating spectrum band is determined, the communication can be performed over this spectrum band. However, if the current spectrum band in use becomes unavailable, the spectrum mobility function is performed to provide a seamless transmission and to avoid possible interference to the licensed users, by switching to another available spectrum holes. Thus, a very flexible signal processing structure is needed to be able to scan a wide spectrum band.

There exists a variety of different methods for spectrum sensing [3]. Following [4] we may arrange these techniques into two groups. In the first group a narrow-band detector is deployed for wide-band spectrum sensing which uses a tunable Band Pass Filter (BPF) at the Radio Frequency (RF) front end and scans one band at a time. Since analog filters are not easily tunable this approach is usually quite expensive, slow, and inflexible since at least two tunable BPF are needed, one for spectrum sensing and a second for the actual signal receiver of the CR unit. In a second approach, the input signal is sampled at Nyquist rate that is twice the highest wide-band frequency. In this approach the analog front-end is fixed and the signal samples can be used for both spectrum sensing as well as for the actual signal receiver of the CR. However, since CR typically operates in a wideband environment this might require a prohibitively large Nyquist sampling rate, and consequently very fast signal processing capability.

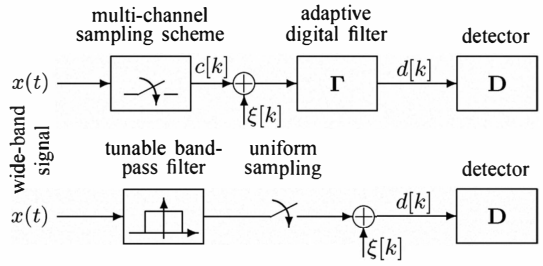

Fig. 1. Sub-Nyquist sampling of a wide-band signal $x(t)$ using a multi-channel scheme and a subsequent digital extraction filter versus band-pass filtering, and uniform sampling.

A promising alternative is the use of sub-Nyquist sampling techniques [5]–[7] and to exploit the fact that the CR only needs to observe a small fraction of the wide-band spectrum at each time. In such a scheme the input signal is sampled with a multichannel sampling scheme with a rate which can be much lower than the Nyquist rate. Afterwards, an adaptive digital filter is used to extract the signal samples of a particular signal band [7] as shown in the upper half of Fig. 1. The advantage is that

- We can sample and process the data on a fairly low rate.
- The digital filter Γ can be adapted easily and fast to different signal bands.
- One can deploy several filters Γ in parallel operating on the same signal samples. For example, one filter may be used for spectrum scanning, another for receiving and extraction the actual data, and a third for monitoring an already detected free band.

In principle, the proposed scheme belongs to the first group of sensing schemes, but using an adaptive digital filter operation on sub-Nyquist (non-uniform) signal samples instead using a tunable bandpass filter (cf. Fig.1). Nevertheless, there also

978-1-61284-074-1/11/$26.00 ©2011 IEEE

exists a major different between the two schemes sketched in Fig.1, namely that the noise (due to, e.g., quantization or thermal noise) is added at different points. Using analog filters, the noise enters just in front of the detector and consequently it can often assumed to be white and uncorrelated. However, in the sub-Nyquist sampling scheme, the additive noise passes the digital filter $\mathbf{\Gamma}$ such that the detector observes the signal in correlated noise.

After our signal model is explained in Section II, Section III explains the sub-Nyquist sampling scheme which is assumed throughout this paper. In Section IV the digital filter is derived which extracts a particular signal band from the sub-Nyquist samples, and Section V compares the energy and the quadratic detector which might be used for sensing. The paper closes with a short summary in Section VI.

II. Signal Model

A. Notations

As usual $L^2(\mathbb{R})$ denotes the Hilbert space of square integrable functions on the real axis $\mathbb{R}$ equipped with the inner product $\langle x, y\rangle = \int_{\mathbb{R}} x(t)\, y(t)\, \mathrm{d}t$ and the corresponding norm. For every $x \in L^2(\mathbb{R})$, the Fourier transform is defined as

$$\widehat{x}(\omega) = \int_{-\infty}^{\infty} x(t)\, \mathrm{e}^{-\mathrm{i}\omega t}\, \mathrm{d}t\,, \quad \omega \in \mathbb{R}\,.$$

Let $\mathbb{B} \subset \mathbb{R}$ be an arbitrary subset of the real axis. Then $PW(\mathbb{B})$ denotes the *Paly-Wiener space* of functions in $L^2(\mathbb{R})$ that are bandlimited to $\mathbb{B}$, i.e.

$$PW(\mathbb{B}) = \{x \in L^2(\mathbb{R}) : \widehat{x}(\omega) = 0 \text{ for all } \omega \notin \mathbb{B}\}\,.$$

Vectors in a finite dimensional Euclidean space $\mathbb{C}^N$ or $\mathbb{R}^N$ are denoted by boldface letters with an overline arrow, like $\vec{\mathbf{c}}$. If $\vec{\mathbf{c}} \in \mathbb{R}^N$ is a random vector with a multivariate Gaussian distribution with mean vector $\vec{\mathbf{m}}$ and covariance matrix $\mathbf{\Sigma}$, then this is denoted by writing $\vec{\mathbf{c}} \sim \mathcal{N}(\vec{\mathbf{m}}, \mathbf{\Sigma})$.

B. Multiband Signal

We assume that the CR units observe a wide spectral range $\mathbb{B}_{\mathrm{WB}}$ in which several primary users may be active. For the following considerations, the whole observed spectral range is subdivided (cf. Fig. 2) into disjoint subintervals $\mathbb{B}_k$ of equal width Ω and center frequencies $\omega_k = \nu_k\, \Omega$ where $\nu_k \in \mathbb{Z}$ lies in the range between $\nu_{\min} = 1$ and $\nu_{\max}$. Thus

$$\mathbb{B}_k := \{\omega \in \mathbb{R} \;:\; \omega_k - \Omega/2 \le \omega < \omega_k + \Omega/2\}$$

and the union of all these subintervals covers the whole spectral range $\mathbb{B}_{\mathrm{WB}} = \bigcup_{k=1}^{\nu_{\max}} \mathbb{B}_k$. For simplicity of exposition, it is assumed that each primary user operates in one of the spectral intervals $\mathbb{B}_k$. The more general case in which the primary users operate in disjoint but arbitrary spectral ranges $\mathbb{B}_k$ can easily lead back to the particular case considered here (see [7] for details).

Now we consider the following transmission and sensing scheme for each CR unit. At each time instant the CR unit is not interested in the whole wideband signal contained in

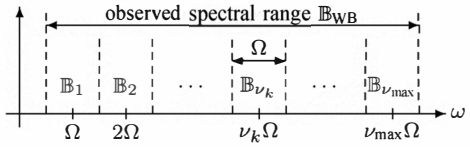

Fig. 2. Partitioning of the observed spectral range into $\nu_{\max}$ disjoint subintervals of width Ω.

$\mathbb{B}_{\mathrm{WB}}$ but only in the signal parts contained in $K < \nu_{\max}$ subbands $\mathbb{B}_{\nu_1}, \ldots, \mathbb{B}_{\nu_K}$. For example, $\mathbb{B}_{\nu_1}$ might be the actual transmission band of the CR unit, $\mathbb{B}_{\nu_2}$ might be a band which was already detected by the CR unit to be free and which is constantly observed as an alternative transmission band if the actual band gets occupied by a primary user. Finally, $\mathbb{B}_{\nu_3}$ might be a band which should actually be sensed whether or not it is free or occupied by a primary user. Additional other band $\mathbb{B}_{\nu_4}, \ldots, \mathbb{B}_{\nu_K}$ for other purposes might be of interest for the CR unit. The set $\mathcal{K} = \{\nu_1, \ldots, \nu_K\}$ of the K integers characterizing the locations of the sub-bands $\mathbb{B}_k$, which are of interest for the CR unit, will be called the *frequency location pattern*. Clearly, this frequency location pattern changes from time to time. For example, if the actual sensing band is detected to be occupied, then the CR unit will switch to another sensing band. Consequently $\mathcal{K}$ will change.

However, for a fixed frequency location pattern the CR units is interested in signals in $x \in \mathbb{B}$ concentrated on a multiband region

$$\mathbb{B} = \bigcup\nolimits_{\nu_k \in \mathcal{K}} \mathbb{B}_{\nu_k}\,. \tag{1}$$

If x is a wideband signal whose Fourier transform is supported in $\mathbb{B}_{\mathrm{WB}}$, then if x would be sampled uniformly at Nyquist rate $\nu_{\max}\Omega/(2\pi)$ it would be easy to extract the desired signal components contained in the spectral band $\mathbb{B}_{\nu_k}$ with $\nu_k \in \mathcal{K}$. However, this may require prohibitively high sampling rates and signal processing capabilities. Therefore, we consider a sub-Nyquist sampling which is described in the next section.

III. Sampling Scheme

We assume that the wideband signal is sampled by a sub-Nyquist multi-channel sampling scheme with N channels as sketched in Fig. 3. Thus, the signal is passes N filters with frequency responses $\widehat{g}^{(n)}$ with a subsequent uniform sampling with a sampling rate $\Omega/2\pi$ proportional to the width of the subintervals $\mathbb{B}_k$. For concreteness we consider only the case where the transfer functions of the filter functions $\widehat{g}^{(n)}$ are given by

$$\widehat{g}^{(n)}(\omega) = \mathrm{e}^{-\mathrm{i}\tau_n \omega}\,, \quad n = 1, \ldots, N$$

and where the delays τ_n have the particular form

$$\tau_n = \delta_n \frac{2\pi}{\nu_{\max}\, \Omega} \tag{2}$$

for some integers $\delta_n \in \{1, 2, \ldots, \nu_{\max}\}$. Such a sampling scheme is usually called *multicoset sampling* and the set $\mathcal{N} =$

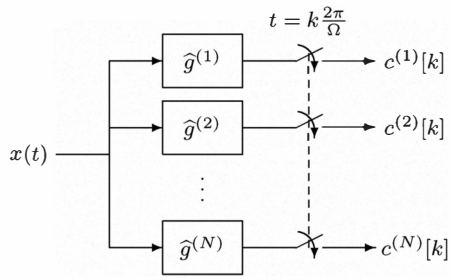

Fig. 3. A general multichannel sampling scheme with N channels.

$\{\delta_n : n = 1, 2, \ldots, N\}$ of the corresponding delay coefficients is refereed to as the *sampling pattern* [8]. The signal at the output of the nth sampling filter is given by

$$y^{(n)}(t) = \frac{1}{2\pi}\int_{\mathbb{B}} \widehat{x}(\omega)\,\widehat{g}^{(n)}(\omega)\,\mathrm{e}^{\mathrm{i}\omega t}\,\mathrm{d}\omega \qquad (3)$$
$$= \frac{1}{2\pi}\int_{-\infty}^{\infty} \widehat{x}(\omega)\,\mathrm{e}^{\mathrm{i}\omega(t-\tau_n)}\,\mathrm{d}\omega = x(t-\tau_n)\ .$$

Thus the filters represent just a delay of the signal by τ_n. Sampling $y^{(n)}$ at a rate of $2\pi/\Omega$ and using that the delays are given by (2), one obtains

$$c^{(n)}[k] := x(k\tfrac{2\pi}{\Omega} - \tau_n) = x(\tfrac{2\pi}{\nu_{\max}\Omega}[k\nu_{max} - \delta_n])$$
$$= x([k\nu_{max} - \delta_n]\,T_{\mathrm{NYQ}})$$

for the signal samples in the nth channel. Therein $1/T_{\mathrm{NYQ}} = \nu_{\max}\Omega/(2\pi)$ is the Nyquist frequency of the wideband signal. The whole sampling scheme is completely determined by the sampling pattern $\mathcal{N}$. Clearly, the sampling pattern can not be chosen arbitrarily. A minimal requirement on $\mathcal{N}$ is, that the signal $x \in PW(\mathbb{B})$ can be reconstructed from the samples $\{c^{(n)}[k]\}$, where $\mathbb{B}$ is the spectral range (1) of the required signal.

To derive a sufficient condition on $\mathcal{N}$ such that this is possible, we first notice from (3) that the signal samples $c^{(n)}[k]$ may be written as

$$c^{(n)}[k] = y^{(n)}(k\tfrac{2\pi}{\Omega}) = \tfrac{1}{2\pi}\langle \widehat{x}, \widehat{s}_k^{(n)}\rangle = \langle x, s_k^{(n)}\rangle$$

where the so-called *sampling functions* $s_k^{(n)}$ are given in the Fourier domain by

$$\widehat{s}_k^{(n)}(\omega) = \chi_{\mathbb{B}}(\omega)\,\exp\left(-\mathrm{i}\tfrac{2\pi}{\nu_{\max}\Omega}\,[k\nu_{\max} - \delta_n]\,\omega\right)\ . \qquad (4)$$

Now, we consider the sampling operator $\mathrm{S} : PW(\mathbb{B}) \to \ell^2$ which maps a signal $x \in PW(\mathbb{B})$ onto the sequence of signal samples

$$\mathrm{S}\ :\ x \mapsto \{c^{(n)}[k] = \langle x, s_k^{(n)}\rangle : n = 1, \ldots, N\ ;\ k \in \mathbb{Z}\}\ .$$

We require that every signal $x \in PW(\mathbb{B})$ can be reconstructed from the samples $\boldsymbol{c} := \{c^{(n)}[k]\}_{k\in\mathbb{Z}}^{n=1,\ldots,N}$ by means of a bounded linear operator. This means that we require that S is bounded and invertible, i.e. we assume that there exists constants $0 < A \le B < \infty$ so that

$$A\,\|x\|^2 \le \|\mathrm{S}x\|^2 \le B\,\|x\|^2 \quad \text{for all} \quad x \in PW(\mathbb{B})\ . \qquad (5)$$

Inserting explicitly the sampling operator S, this condition is equal to

$$A\,\|x\|^2 \le \sum_{n=1}^{N}\sum_{k\in\mathbb{Z}} |\langle x, s_k^{(n)}\rangle|^2 \le B\,\|x\|^2$$

which shows that this condition is equivalent to require that the sequence $\{s_k^{(n)}\}$ forms a frame for the signal space $PW(\mathbb{B})$, and the constants A and B are the so-called frame bounds [9].

Necessary and sufficient conditions for $\{s_k^{(n)}\}$ to be a frame for $PW(\mathbb{B})$ are derived in [7] for arbitrary filter functions $\widehat{g}^{(n)}$. For the special case of the multicoset sampling scheme, these conditions can be formulated as follows.

Lemma 1: *Let $\mathbb{B}$ be a multiband region with K bands and with the location pattern $\mathcal{K} = \{\nu_1, \ldots, \nu_K\}$, and let $\mathcal{N} = \{\delta_1, \ldots, \delta_N\}$ be the sampling pattern of a multicoset sampling scheme. Denote by $\mathbf{H}$ the $K \times N$ matrix with entries*

$$[\mathbf{H}]_{k,n} = \exp\left(-\mathrm{i}\,2\pi\frac{\nu_k\,\delta_n}{\nu_{\max}}\right)\ .$$

Then the sequence $\{s_k^{(n)}\}_{k\in\mathbb{Z}}^{n=1,\ldots,N}$ of sampling functions defined by (4) forms a frame for $PW(\mathbb{B})$ if and only if there exists constants $0 < \alpha \le \beta < \infty$ such that

$$\alpha\mathbf{I}_K \le \mathbf{H}\,\mathbf{H}^* \le \beta\mathbf{I}_K\ . \qquad (6)$$

It form a Riesz basis for $PW(\mathbb{B})$ if and only if additionally $N = K$. Moreover, the lower and upper frame bounds are given by

$$A = \tfrac{\Omega}{2\pi}\,\lambda_{\min}(\mathbf{H}\,\mathbf{H}^*) \quad \textit{and} \quad B = \tfrac{\Omega}{2\pi}\,\lambda_{\max}(\mathbf{H}\,\mathbf{H}^*)\ . \qquad (7)$$

The upper bound in (6) is always be satisfied since $\mathbf{H}\,\mathbf{H}^*$ has a finite size of $K \times K$. Thus Lemma 1 basically requires that the $K \times N$ matrix $\mathbf{H}$ has rank K. To this end, it is necessary that $N \ge K$, i.e. the number N of channels in the sampling bank of Fig. 3 has to be at last equal to the number of signal band K. Situations in which $N > K$ correspond to an oversampling of the signal.

So given the band location pattern $\mathcal{K} = \{\nu_1, \ldots, \nu_K\}$ the sampling pattern $\mathcal{N} = \{\delta_1, \ldots, \delta_N\}$ has to be chosen such that (6) is satisfied. Nevertheless, it is easy to see that there exist *universal sampling patters* $\mathcal{N}$ such that $\mathbf{H}$ has rank K irrespective of the band locations $\mathcal{K}$. The pattern $\mathcal{N}_0 = \{\delta_1 = 1, \delta_2 = 2, \ldots \delta_N = N\}$ is an example [8], [10] since in this case $\mathbf{H}$ is a Vandermonde matrix for any choice of $\mathcal{K}$. Nevertheless, the frame bounds A and B still depend strongly both, on the band locations $\mathcal{K}$ as well as on the sampling pattern $\mathcal{N}$. Since these frame bounds influence the stability behavior of the sampling scheme, the sampling pattern $\mathcal{N}$ should be chosen such that these frame bounds are optimized in a certain sense. This problem is discussed next.

A. Robustness of the Sampling Scheme

If the sampling pattern $\mathcal{N}$ satisfies the conditions of Lemma 1 then the sampling functions $\{s_k^{(n)}\}$ form a frame with frame bounds A and B. Consequently, the corresponding sampling operator $\mathrm{S} : PW(\mathbb{B}) \to \ell^2$ satisfies (5), which

shows that S is bounded and bounded below such that there exists a bounded inverse $\mathrm{S}^{-1} : \ell^2 \to PW(\mathbb{B})$ with $\|\mathrm{S}^{-1}\| = 1/\sqrt{A} < \infty$. In other words, $\mathrm{S}^{-1} : \boldsymbol{c} \mapsto x$ is a bounded linear operator which reconstructs the signal x from its samples $\boldsymbol{c}$. However, the robustness of this reconstruction, with respect to disturbances in the signal samples, is determined by the *condition number* B/A of the sampling scheme.

To see this, let $\boldsymbol{c} = \mathrm{S}x$ be the sequence of samples of an arbitrary $x \in PW(\mathbb{B})$ and assume that these samples are contaminated by additive sample noise as

$$\widetilde{c}^{(n)}[k] = c^{(n)}[k] + \xi^{(n)}[k] \,, \quad k \in \mathbb{Z} \,, \; n = 1, \ldots, N \,.$$

Therein $\boldsymbol{\xi} = \{\xi^{(n)}[k]\}$ is an ℓ^2-sequence which models the error, e.g. due to quantization or thermal noise. The ratio $SNR = \|\boldsymbol{c}\|^2/\|\boldsymbol{\xi}\|^2$ is the signal-to-noise ratio of the sampling scheme. Now the signal is reconstructed based on the erroneous samples $\widetilde{\boldsymbol{c}}$. By the linearity of S^{-1}, one obtains

$$\widetilde{x} := \mathrm{S}^{-1}\widetilde{\boldsymbol{c}} = \mathrm{S}^{-1}\boldsymbol{c} + \mathrm{S}^{-1}\boldsymbol{\xi} = x + \mathrm{S}^{-1}\boldsymbol{\xi}$$

for the reconstructed signal. Therewith, the relative reconstruction error can be upper bounded by

$$\frac{\|x - \widetilde{x}\|^2}{\|x\|^2} = \frac{\|\mathrm{S}^{-1}\boldsymbol{\xi}\|^2}{\|x\|^2} \leq \frac{B}{A}\frac{\|\boldsymbol{\xi}\|^2}{\|\boldsymbol{c}\|^2} = \frac{B}{A}\frac{1}{SNR} \,. \qquad (8)$$

This upper bound is tight, i.e. there are signals $x \in PW(\mathbb{B})$ and noise sequences $\boldsymbol{\xi} \in \ell^2$ so that equality holds in (8). Since $A > 0$ the reconstruction error is always finite and can be made arbitrarily small by increasing the SNR. Therefore, the sampling scheme is said to be *stable*. However, since the upper bound increases proportional with the condition number B/A, a sampling scheme with a large condition number is less robust against errors in the samples. For this reason, the sampling pattern $\mathcal{N}$ should be chosen such that B/A is as small as possible.

Example 1: We consider a configuration with $K = 3$ signal bands with band location pattern $\mathcal{K} = \{\nu_1, \nu_2, \nu_3\}$, where every ν_k lies in the range from $\nu_{\min} = 1$ to $\nu_{\max} = 50$. For illustration, we fix $\nu_1 = 10$ and $\nu_2 = 40$ and vary only ν_3. Then we apply the universal sampling pattern $\mathcal{N}_0$ with $N = 3$ and with $N = 4$ sampling filters and determine for every ν_3 the condition number B/A. The result is shown in Fig. 4 on a logarithmic scale. It shows that if the third band ν_3 lies close to one of the other bands, then the condition number becomes very high, i.e. the sampling scheme becomes almost unstable. For comparison, Fig. 4 also shows the condition number for the optimal sampling pattern $\mathcal{N}_{\text{opt}}$, i.e. the sampling pattern $\mathcal{N}$ which yields the lowest condition number for the actual band location pattern $\mathcal{K}$. It is clear to see that an adaption of the sampling pattern $\mathcal{N}$ to the actual band locations $\mathcal{K}$ yields a massive improvement in terms of robustness, compared to the universal sampling pattern, in most of the cases. Fig. 4 also illustrates that oversampling ($N = 4$) gives a noticeable improvement in terms of the condition number. Nevertheless, the universal sampling pattern is still much worse than the optimized one, for almost all band locations.

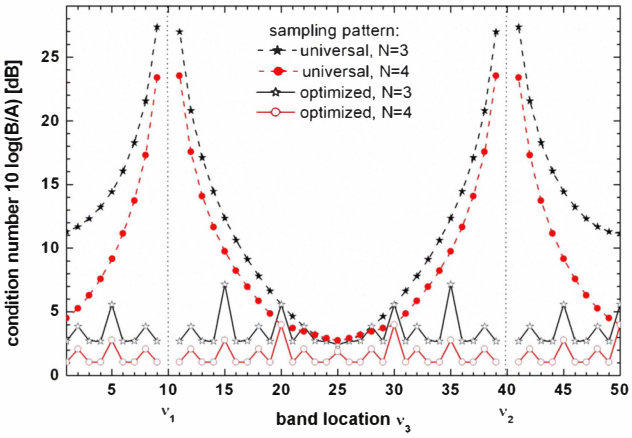

Fig. 4. Condition number of a multicoset sampling scheme as function of the band location ν_3 for signals with $K = 3$ frequency bands and for sampling schemes with $N = 3$ and $N = 4$ sampling filters.

Note that the poor behavior of the universal sampling pattern, as illustrated in the previous example, is prototypical. This follows from results in [11] where the eigenvalues of matrices like $\mathbf{H}\mathbf{H}^*$ where studied in detail. Consequently, whenever possible, the sampling pattern should always be adapted to the actual band locations.

IV. Digital Extraction Filter

This section gives the transfer function of the digital filter $\mathbf{\Gamma}_q$, which is used to extract the required signal samples corresponding to a signal in the required signal band from the multicoset samples of the wideband signal. Due to the limited space, we only present the result here. For an elaborated derivation, we refer to [7].

A. Required Signal Samples

Sampling a multiband signal $x \in PW(\mathbb{B})$ with a multicoset sampling scheme as described in the Sec. III, gives N sequences $\{c^{(n)}[k] = \langle x, s_k^{(n)} \rangle\}_{k \in \mathbb{Z}}$, $n = 1, \ldots, N$ of uniform samples of x. If the conditions of Lemma 1 are satisfied, we are able to reconstruct the signal $x \in PW(\mathbb{B})$ from these samples. However, our primarily aim is not to reconstruct the whole signal x, but only to determine the signal samples corresponding to one of the multiband components, say $\mathbb{B}_{\nu_q}$ with $\nu_q \in \mathcal{K}$. So we are interested in the samples of the down-converted and low-pass filtered signal

$$y(t) = \frac{1}{2\pi}\int_{-\infty}^{\infty} \widehat{x}(\omega + \omega_q)\,\overline{\widehat{F}(\omega)}\,\mathrm{e}^{\mathrm{i}\omega t}\,\mathrm{d}\omega$$

where $\omega_q = \nu_q\Omega$ is the center frequency of the required signal band, and where $\widehat{F}$ denotes the frequency response of the low-pass filter (cf. Fig. 5). Here we assume that F is an ideal lowpass matched to the required frequency band $\mathbb{B}_q$, i.e. $\widehat{F}(\omega) = \chi_{\mathbb{B}_q}(\omega)$. Afterwards this filtering signal is sampled with a rate $\Omega/(2\pi)$ which gives the required samples of $y(t)$

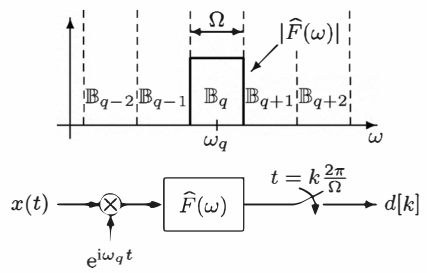

Fig. 5. Required sample sequence $\{d[k]\}_{k\in\mathbb{Z}}$, after down-conversion, low-pass filtering, and uniform sampling of the multiband signal $x(t)$.

at time instances $t = k\,\frac{2\pi}{\Omega}$ as

$$d[k] = y\left(k\,\tfrac{2\pi}{\Omega}\right) = \tfrac{1}{2\pi}\,\langle \widehat{x}, \widehat{w}_k\rangle = \langle x, w_k\rangle\ , \quad k \in \mathbb{Z}$$

with the so called *reconstruction functions*

$$w_k(t) = w\left(t - k\tfrac{2\pi}{\Omega}\right)\ , \quad k \in \mathbb{Z} \tag{9}$$

where $w(t) = F(t)\,e^{i\omega_q t}$. In the frequency domain these functions are given by $\widehat{w}_k(\omega) = \widehat{w}(\omega)\,e^{-ik\frac{2\pi}{\Omega}\omega}$ with the function $\widehat{w}(\omega) = \widehat{F}(\omega-\omega_q) = \chi_{\mathbb{B}_q}(\omega-\omega_q)$.

B. Extraction Filter

Given the samples $\boldsymbol{c} = \{c^{(n)}[k] = \langle x, s_k^{(n)}\rangle\}_{k\in\mathbb{Z}}^{n=1,\dots,N}$ of a multiband signal x, we seek a digital filter $\boldsymbol{\Gamma}_q$ which determines the required samples $d[m] = \langle x, w_m\rangle$ of a certain multiband component $\mathbb{B}_q$. We require that $\boldsymbol{\Gamma}_q$ is linear. Consequently, it has the form

$$\begin{aligned} d[m] = (\Gamma_q\,\boldsymbol{c})[m] &= \sum_{k\in\mathbb{Z}}\sum_{n=1}^{N} \gamma_k^{(n)}\,c^{(n)}[m-k] \\ &= \sum_{k\in\mathbb{Z}} \boldsymbol{\gamma}_k^{\mathrm{T}}\,\mathbf{c}_{m-k} \end{aligned} \tag{10}$$

with a coefficient sequence $\{\gamma_k^{(n)}\} \in \ell^2$, and where we defined $\boldsymbol{\gamma}_k^{\mathrm{T}} := (\gamma_k^{(1)},\dots,\gamma_k^{(N)})$ and $\mathbf{c}_k := (c_k^{(1)},\dots,c_k^{(N)})^{\mathrm{T}}$. As usual

$$\boldsymbol{\Gamma}_q(e^{i\theta}) := \textstyle\sum_{k\in\mathbb{Z}} \boldsymbol{\gamma}_k\,e^{ik\theta} \tag{11}$$

is called the *transfer function* of the linear filter (10).

Lemma 2: *Let $\mathcal{K} = \{\nu_1,\dots,\nu_K\}$ be a given band location pattern, and let $\mathcal{N} = \{\delta_1,\dots,\delta_N\}$ be a corresponding sampling pattern which satisfies the condition of Lemma 1. Assume that we want to extract the samples of the band $\mathbb{B}_{\nu_q}$ with index $\nu_q \in \mathcal{K}$. Then the transfer function of the filter $\boldsymbol{\Gamma}_q$ which determines the sample $\{d[k]\}$ form the samples $\boldsymbol{c} = \{c^{(n)}[k]\}$ is given by*

$$\boldsymbol{\Gamma}_q(e^{i\theta}) = \mathbf{D}(e^{i\theta})\,\mathbf{A}^{\dagger}\,\mathbf{w} = \mathbf{D}(e^{i\theta})\,\overline{\mathbf{H}}^{\dagger}\,\mathbf{e}_q \tag{12}$$

where $\mathbf{D}(e^{i\theta})$ is a unitary $N\times N$ diagonal matrix whose entries are given by

$$[\mathbf{D}(e^{i\theta})]_{n,n} = \exp\left(\mathrm{i}\,\frac{\delta_n\,\theta}{\nu_{\max}}\right)\ , \tag{13}$$

where $\mathbf{A} = \overline{\mathbf{H}^*\mathbf{H}}$ is a constant self adjoint $N\times N$ matrix with entries

$$[\mathbf{A}]_{n,m} = \textstyle\sum_{k=1}^{K} \exp\left(-\mathrm{i}\,2\pi\,\frac{\delta_n-\delta_m}{\nu_{\max}}\,\nu_k\right)\ ,$$

and where $\mathbf{w}$ is a constant length N vector with entries

$$[\mathbf{w}]_n = \exp(-\mathrm{i}\,2\pi\,\delta_n\nu_q/\nu_{\max})\ .$$

Remark 1: Note that $\mathbf{w}$ is just the qth column of $\mathbf{H}^{\mathrm{T}}$, i.e. $\mathbf{w} = \mathbf{H}^{\mathrm{T}}\,\mathbf{e}_q$ where $\mathbf{e}_q$ is the qth identity vector in $\mathbb{C}^K$. This observation yields the right hand side equation of (12).

A proof of this result may be found in [7]. There, the above result was derived for a much more general situation and the above lemma only represents a particular case. Moreover, [7] also derived an optimal causal filter $\boldsymbol{\Gamma}_q$ which only uses past signal samples $\{c^{(n)}[k]\}_{k\le m}^{n=1,\dots,N}$ to determine an estimate of $d[m]$.

Given the transfer function (12) of the correction filter, it is easy to determine the coefficients $\gamma_k^{(n)}$ of the linear filter (10):

$$\begin{aligned} \boldsymbol{\gamma}_k &= \frac{1}{2\pi}\int_{-\pi}^{\pi} \boldsymbol{\Gamma}_q(e^{i\theta})\,e^{-ik\theta}\,d\theta \\ &= \frac{1}{2\pi}\int_{-\pi}^{\pi} \mathbf{D}(e^{i\theta})\mathbf{A}^{\dagger}\,\mathbf{w}(e^{i\theta})\,e^{-ik\theta}\,d\theta \\ &= \mathbf{D}_k\,\mathbf{A}^{\dagger}\,\mathbf{w} = \mathbf{D}_k\,\overline{\mathbf{H}}^{\dagger}\,\mathbf{e}_q \end{aligned}$$

wherein $\mathbf{D}_k$ is an $N\times N$ diagonal matrix with entries

$$[\mathbf{D}_k]_{n,n} = \frac{\sin([\delta_n/\nu_{max}-k]\pi)}{[\delta_n/\nu_{max}-k]\pi}\ .$$

Generally, the impulse response of the filter $\boldsymbol{\Gamma}_q$ extends from ∞ to ∞. However, in practice this infinite impulse response has to be truncated at some point. Therefore, we assume in the following that the filter (10) is truncated at a certain index L such that

$$d[m] = \sum_{k=-L}^{L}\sum_{n=1}^{N} \gamma_k^{(n)}\,c^{(n)}[m-k]\ . \tag{14}$$

Therewith, we derived the digital filter which extracts the signal samples of a particular multiband component $\mathbb{B}_\nu$ from the signal samples obtained with a multicoset sampling scheme. Of course, one may apply several of these filters in parallel to extract multiple signal components, e.g. one filter to extract the actual transmission band, and another to extract the actual sensing band, and so on.

V. Sensing

There are several publications which investigate detectors for uncorrelated noise but for different probability distributions of the noise in cognitive radio context [3], [13], [14].

In this section we are in particular interested in the sensing band, i.e. we assume that $\mathbb{B}_{\nu_q}$ is the actual sensing band and that the filter $\boldsymbol{\Gamma}_q$ extracts the signal samples of this band. Consequently, we have a situation as shown at the top of Fig. 1 where $\{d[k]\}$ represents the sequence of signal samples in the actual sensing band. Based on these signal samples we want to

decide whether the signal band $\mathbb{B}_q$ is occupied or not. To this end, the CR unit observes M consecutive samples $\{d[k]\}_{k=1}^{M}$ at the output of the extraction filter $\mathbf{\Gamma}_q$, which can be written as

$$\begin{aligned} d[k] &= (\mathbf{\Gamma}_q \boldsymbol{c})[k] + (\mathbf{\Gamma}_q \boldsymbol{\xi})[k] \\ &= s[k] + \eta[k]\,, \quad k = 1, 2, \ldots, M \end{aligned} \tag{15}$$

where $\boldsymbol{\xi} = \{\xi^{(n)}[k]\}_{k\in\mathbb{Z}}$ is again a noise sequence which is assumed to consists of independent, identical, normal distributed random variables with zero mean and variance σ_ξ^2. The sequence $\{s[k] = (\mathbf{\Gamma}_q\, \boldsymbol{c})[k]\}$ contains the signal samples in the band $\mathbb{B}_{\nu_q}$. In general, the statistical properties of these samples are unknown, and they may be multiplied with a certain complex number representing the attenuation and phase shift introduced by the communication channel. Nevertheless, in the following we assume that the samples $s[k]$ are normal distributed random variables with zero mean. This assumption is motivated by the fact that normal distributed random variable have maximal entropy and can achieve a maximum data rate. Therefore decoding schemes in communications often try to approximate such an distribution of the data.

The $M+1$ consecutive samples, observed by the CR unit, are collected[1] in the vector

$$\vec{\mathbf{d}} = (d[m], d[m+1], \ldots, d[m+M])^{\mathrm{T}}\ .$$

Using (14) and (15) this vector is obtained by

$$\vec{\mathbf{d}} = \mathbf{G}\,\vec{\mathbf{c}} + \mathbf{G}\,\vec{\boldsymbol{\xi}} = \vec{\mathbf{s}} + \vec{\boldsymbol{\eta}}\,. \tag{16}$$

Therein $\vec{\mathbf{c}}$ and $\vec{\boldsymbol{\xi}}$ are vectors of length $N(2L+M+1)$ containing the samples $\{c^{(n)}[k]\}$ and the sample noise $\{\xi^{(n)}[k]\}$ as follows

$$\vec{\mathbf{c}} = (\vec{\mathbf{c}}^{(1)}, \vec{\mathbf{c}}^{(2)}, \ldots, \vec{\mathbf{c}}^{(N)})^{\mathrm{T}}$$

with

$$\vec{\mathbf{c}}^{(n)} = (c^{(n)}[m-L], c^{(n)}[m-L+1], \ldots, c^{(n)}[m+M+L])^{\mathrm{T}}$$

and analogous for $\vec{\boldsymbol{\xi}}$. The matrix $\mathbf{G}$ contains the filter coefficients of the filter (14). It has size $(M+1)\times N(2L+M+1)$ and the form

$$\mathbf{G} = (\mathbf{G}^{(1)}, \mathbf{G}^{(2)}, \ldots, \mathbf{G}^{(N)})^{\mathrm{T}}$$

wherein each $\mathbf{G}^{(n)}$ is an $(M+1)\times(2L+M+1)$ Toeplitz matrix given by

$$\mathbf{G}^{(n)} = \begin{pmatrix} \gamma_L^{(n)} & \cdots & \gamma_0^{(n)} & \cdots & \gamma_{-L}^{(n)} & & \\ & \ddots & & & & \ddots & \\ & & \gamma_L^{(n)} & \cdots & \gamma_0^{(n)} & \cdots & \gamma_{-L}^{(n)} \end{pmatrix}\ .$$

Thus the detector observes (16) where $\vec{\mathbf{s}} \sim \mathcal{N}(0, \mathbf{\Sigma}_s)$ and $\vec{\boldsymbol{\eta}} \sim \mathcal{N}(0, \mathbf{\Sigma}_\xi)$. According to the above assumptions on the sample noise $\xi^{(n)}[k]$ the corresponding covariance matrix is given by $\mathbf{\Sigma}_\eta = \sigma_\xi^2 \mathbf{G}\,\mathbf{G}^{\mathrm{T}}$. If no further information on the signal samples $s[k]$ are available, we may assume that $\mathbf{\Sigma}_s = \sigma_s^2 \mathbf{I}_{M+1}$. Based on the observation (16), the detector has to decide between the two hypotheses

$$\mathcal{H}_0 : \vec{\mathbf{d}} = \vec{\boldsymbol{\eta}} \qquad \text{and} \qquad \mathcal{H}_1 : \vec{\mathbf{d}} = \vec{\mathbf{s}} + \vec{\boldsymbol{\eta}} \tag{17}$$

i.e. between the hypothesis $\mathcal{H}_0$ that a signal is absent and the hypothesis $\mathcal{H}_1$ that a signal is present.

A. Energy detector

The most simple form of an detector is a so called energy detector. Such a detector simply calculates the energy of the received signal $\vec{\mathbf{d}}$

$$E_{\mathbf{d}} = \sum_{m=1}^{M+1} |d_m|^2$$

and compares this quantity with a certain threshold τ. If $E_{\mathbf{d}} < \tau$ the detector would decide for $\mathcal{H}_0$ otherwise for $\mathcal{H}_1$. The threshold τ is chosen, such that a certain desired probability of false alarm is obtained. Clearly, the threshold will be influenced by the noise variance as well as by the number $M+1$ of observed observation sampled.

B. Quadratic Detector

The energy detector does not take into account the correlation of the noise, characterized by $\mathbf{\Sigma}_\eta$, and the possible correlation of the signal samples, characterized by $\mathbf{\Sigma}_s$. However, incorporating this information into the detector design will improved its performance.

To this end, the detector first applies a prewhitening by multiplying $\vec{\mathbf{d}}$ with the matrix $\mathbf{P} = (\mathbf{G}\,\mathbf{G}^{\mathrm{T}})^{-1/2}$:

$$\vec{\mathbf{g}} = \mathbf{P}\,\vec{\mathbf{d}} = \mathbf{P}\,\vec{\mathbf{s}} + \mathbf{P}\,\vec{\boldsymbol{\eta}} = \vec{\mathbf{r}} + \vec{\mathbf{n}}\,. \tag{18}$$

this yields $\vec{\mathbf{r}} = \mathbf{P}\,\vec{\mathbf{s}} \sim \mathcal{N}(0, \mathbf{\Sigma}_r)$ with the covariance matrix

$$\mathbf{\Sigma}_r = \mathbf{P}\,\mathbf{\Sigma}_s\,\mathbf{P}^{\mathrm{T}} = (\mathbf{G}\mathbf{G}^{\mathrm{T}})^{-1/2}\,\mathbf{\Sigma}_s\,(\mathbf{G}\mathbf{G}^{\mathrm{T}})^{-1/2} \tag{19}$$

and $\vec{\mathbf{n}} = \mathbf{P}\vec{\boldsymbol{\eta}} \sim \mathcal{N}(0, \mathbf{\Sigma}_n)$ with $\mathbf{\Sigma}_n = \mathbf{P}\mathbf{\Sigma}_\eta\mathbf{P}^{\mathrm{T}} = \sigma_\xi^2\,\mathbf{I}_{M+1}$. Thus, the noise vector $\vec{\mathbf{n}}$ consists now of uncorrelated white Gaussian noise, and the two hypothesis (17) are equivalent to

$$\mathcal{H}_0 : \vec{\mathbf{g}} = \vec{\mathbf{n}} \qquad \text{and} \qquad \mathcal{H}_1 : \vec{\mathbf{g}} = \vec{\mathbf{r}} + \vec{\mathbf{n}}\,.$$

For such a hypothesis testing problem of a stochastic Gaussian signal $\vec{\mathbf{r}}$ in uncorrelated Gaussian noise $\vec{\mathbf{n}}$, it is known (see, e.g.,[12, Chap. III]) that the optimal decision rule is the so called quadratic detector. Using the prewhitened receive signal $\vec{\mathbf{g}}$, it calculates the quadratic form

$$D = \vec{\mathbf{g}}^{\mathrm{T}}\,\mathbf{Q}\,\vec{\mathbf{g}} \quad \text{with } \mathbf{Q} = \sigma_\xi^{-2}\,\mathbf{I} - (\sigma_\xi^2\,\mathbf{I} + \mathbf{\Sigma}_r)^{-1}$$

and compares it with with a certain threshold τ which is chosen to achieve a nominal probability of false alarm. The quadratic form $\mathbf{Q}$ depends essentially on the covariance matrix $\mathbf{\Sigma}_r$, given in (19), i.e. it depends on the covariance of the actual signal $\vec{\mathbf{s}}$ and on the coefficients of the extraction filter $\mathbf{\Gamma}_q$ which are contained in the matrix $\mathbf{G}$. If $\mathbf{\Sigma}_r$ would be proportional to the identity matrix, the quadratic detector reduces to a simple

[1] In the following, all variables are assumed to be real valued. This assumption is only made for easy of notation. The complex case can be handled by resolve every complex number into its real and imaginary part.

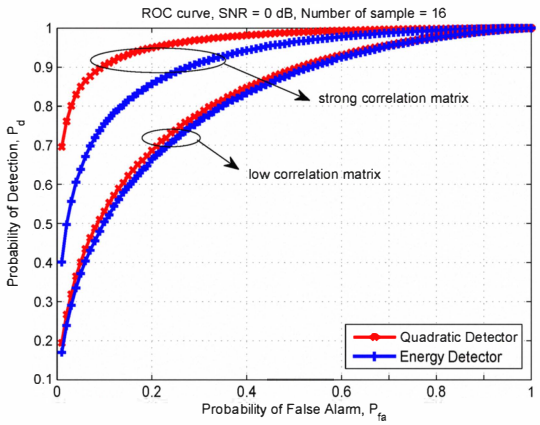

Fig. 6. Comparison of the quadratic detector, taking into count the signal correlation, with an energy detector.

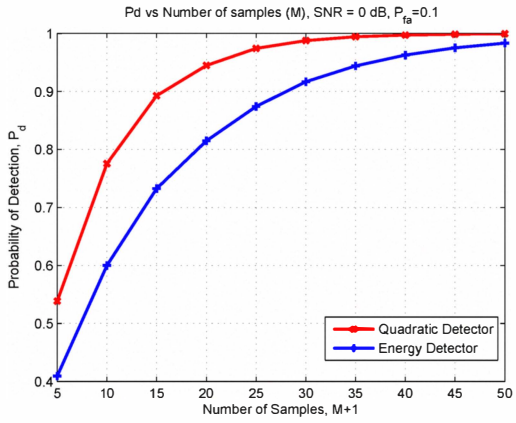

Fig. 7. Probability of detection P_d as a function of observation length $M+1$ for strong correlation signal

energy detector. However, in our situation $\mathbf{\Sigma}_r$ is generally not the identity matrix due to the filter $\mathbf{\Gamma}_q$ which extract the sensing band from the multiband samples $\boldsymbol{c}$, even if the signal $\vec{\mathbf{s}}$ would be uncorrelated.

C. Numerical Examples

To study the influence of the correlation matrix $\mathbf{\Sigma}_r$, we performed simulations using 10^5 monte carlo runs with a correlation matrix of the form

$$\mathbf{\Sigma_r} = \begin{pmatrix} 1 & \rho_1 & \cdots & \rho_{M-1} & \rho_M \\ \rho_1 & 1 & \rho_1 & \cdots & \rho_{M-1} \\ \vdots & \rho_1 & 1 & \ddots & \vdots \\ \rho_{M-1} & \vdots & \ddots & \ddots & \rho_1 \\ \rho_M & \rho_{M-1} & \cdots & \rho_1 & 1 \end{pmatrix}.$$

For a *strong correlation* situation the coefficients ρ_1, ρ_2, ρ_3 are chosen to be equal to $0.3, 0.2, 0.1$ respectively. For a *low correlation* situation we choose $0.03, 0.02, 0.01$. All other correlation coefficients ρ_m with $m > 3$ are always set equal to zero.

Fig. 6 depicts receiver operating characteristics (ROC) curves for both the energy detector and the quadratic detector which are implemented in our scheme. It shows that the improvement of a quadratic detector compared with the energy detector will be larger for stronger correlated signal. In the strong correlation case, at a probability of false alarm of $P_{\mathrm{fa}} = 0.1$, the usage of the quadratic detector in our scheme will increase the probability of detection from around $P_{\mathrm{d}} = 0.7$ to $P_{\mathrm{d}} = 0.9$ compared with the energy detector. This improvement signifies that for a certain capacity of cognitive radio (indicated by deciding correctly the existence of spectrum holes with probability $1 - P_{fa} = 0.9$ for a certain band), the degree of interferences to the licensed users decreases from around 30% to 10%.

Clearly, the performance of the detector for a certain SNR depends also strongly on the observation time M as longer the observation time as better becomes the detector performance as shown in Fig. 7. Meanwhile, one cannot increase the observation time as large as possible in order to increase the performance of the detector, since it will increase overall channel detection time and further will reduce the capacity of the cognitive radio. Referring to IEEE 802.22 wireless regional area network, which is the first cognitive-radio based wireless standard that uses television band (analog tv, digital tv, and wireless microphone), the required channel detection has to be less equal to 2 sec [15], [16].

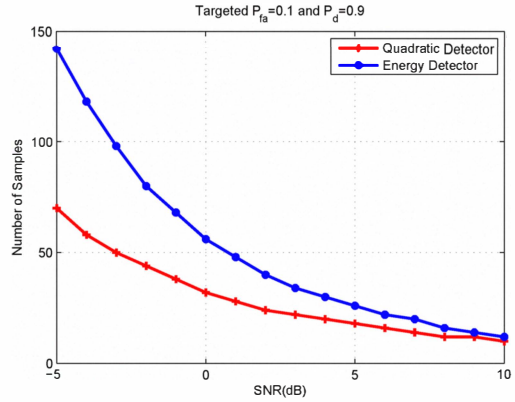

Fig. 8. Minimal necessary observation length for a probability of detection of $P_{\mathrm{d}} = 0.9$ by a probability of false alarm of $P_{\mathrm{fa}} = 0.1$.

Fig. 8 compares minimal observation length or number of samples as a function of SNR for both detectors under strong correlation signal to obtain targeted probability of detection $P_d = 0.9$ and probability of false alarm $P_f = 0.1$. It suggests that it is better to use the quadratic detector rather than energy detector in our scheme to obtain lower detection time. As an example, in relation with IEEE 802.22 standard for detecting analog television band, in order to attain receiver sensitivity -94 dBm with corresponding $SNR = 1$ dB [16], the energy detector requires 48 samples which are almost double of the number of samples for quadratic detector which is only 28. In that case, the quadratic detector is more favorable.

Assume that signals $\vec{s}$ are uncorrelated, i.e. $\mathbf{\Sigma}_s = \sigma_s \mathbf{I}_{M+1}$. Then the correlation matrix (19) is completely determined by the coefficients $\{\gamma_k^{(n)}\}$ of the extraction filter (14) such that $\mathbf{\Sigma}_r$ can explicitly calculate for given band locations and for a given sampling scheme, i.e. for given band location pattern $\mathcal{K} = \{\nu_1, \ldots, \nu_K\}$ and for a chosen sampling pattern $\mathcal{N} = \{\delta_1, \ldots, \delta_N\}$ (cf. the derivation in Section IV-B). This was done for the setup as considered in Example 1. It turned out, that the corresponding correlation matrix $\mathbf{\Sigma}_r$ lies always between the low correlation and the strong correlation case, considered above, depended on the band location and sampling pattern, on the degree L of the filter (14) as well as on the observation length $M + 1$.

VI. Conclusions

This paper proposed a signal processing architecture for cognitive radio applications based on a sub-Nyquist sampling scheme. A digital filter was derived which extracts a particular transmission band from the sub-Nyquist samples, and it was shown that the robustness of this structure with respect to sample noise depends strongly on the chosen sampling pattern. Consequently, the sampling scheme should always be adapted to the actual band locations.

In the second part, we investigated two detectors, which may be applied for sensing the spectrum based on our signal processing scheme, namely an energy detector and a quadratic detector. We present numerical examples to compare these detectors which are implemented in our scheme. It is shown that the performance improvement of the quadratic detector compared with the energy detector will be larger for stronger correlated signal at the output of the prewhitening filter. Furthermore, our simulation result shows that the quadratic detector has the advantage of smaller number of samples than the energy detector for a certain targeted P_{fa} and P_d. It signifies that the quadratic detector will have smaller channel detection time and lower receiver sensitivity than the energy detector and will possibly improve overall system capacity of the cognitive radio. With these results, it is more favorable to use the quadratic detector than the energy detector in our complete scheme.

VII. Acknowledgment

This collaborative work was supported by German Research Foundation or Deutsche Forschungsgemeinschaft (DFG).

References

[1] S. Haykin, "Cognitive radio: brain-empowered wireless communications," *IEEE J. Sel. Areas Commun.*, vol. 23, no. 2, pp. 201–220, Feb. 2005.

[2] Z. Qing and B. M. Sadler, "A Survey of Dynamic Spectrum Access," *IEEE Signal Process. Mag.*, vol. 24, no. 3, pp. 79–89, May 2007.

[3] T. Yücek and H. Arslan, "A survey of spectrum sensing algorithms for cognitive radio applications," *IEEE Commun. Surveys Tuts.*, vol. 11, no. 1, pp. 116–130, 2009.

[4] M. Mishali and Y. C. Eldar, "Wideband Spectrum Sensing at sub-Nyquist Rates," *IEEE Trans. Signal Process.*, 2010, available online at arXiv 1009.1305.

[5] R. Venkataramani and Y. Bresler, "Optimal Sub-Nyquist Nonuniform Sampling and Reconstruction for Multiband Signals," *IEEE Trans. Signal Process.*, vol. 49, no. 10, pp. 2301–2313, Oct. 2001.

[6] M. Mishali and Y. C. Eldar, "From Theory to Practice: Sub-Nyquist Sampling of Sparse Wideband Analog Signals," *IEEE J. Sel. Topics Signal Process.*, vol. 4, no. 2, pp. 375–391, Apr. 2010.

[7] V. Pohl, "Causal Filtering and Signal Extraction from Sub-Nyquist Samples of Multiband Signals," *IEEE Trans. Signal Process.*, 2010, sub. for pub.

[8] R. Venkataramani and Y. Bresler, "Perfect Reconstruction Formulas and Bounds on Aliasing Error in Sub-Nyquist Nonuniform Sampling of Multiband Signals," *IEEE Trans. Inf. Theory*, vol. 46, no. 6, pp. 2173–2183, Sep. 2000.

[9] O. Christensen, *An Introduction to Frames and Riesz Bases.* Bosten: Birkhäuser, 2003.

[10] M. Mishali and Y. C. Eldar, "Blind Multiband Signal Reconstruction: Compressed Sensing for Analog Signals," vol. 57, no. 3, pp. 993–1009, Mar. 2009.

[11] P. J. S. G. Ferreira, "The Eigenvalues of Matrices that Occur in Certain Interpolation Problems," *IEEE Trans. Signal Process.*, vol. 45, no. 8, pp. 2115–2120, Aug. 1997.

[12] H. V. Poor, *An Introduction to Signal Detection and Estimation*, 2nd ed. New York, etc.: Springer, 1994.

[13] M. Ghogho, M. Cardenas-Juarez, A. Swami, and T. Whitworth, "Locally optimum detection for spectrum sensing in cognitive radio," in *Proc. of the 4th IEEE Intern. CROWNCOM Conf.*, Hanover, Germany, Jun. 2009.

[14] F. Y. Suratman, Y. Chakhchoukh, and A. M. Zoubir, "Locally Optimum Detection in Heavy-Tailed Noise for Spectrum Sensing in Cognitive Radio," in *Proc. of the 2nd International Workshop on Cognitive Information Processing (CIP)*, Elba, Italy, Jun. 2010.

[15] C. Cordeiro, K. Challapali, and D. Birru, "IEEE 802.22: An Introduction to the First Wireless Standard based on Cognitive Radios," in *Journal of Communications*, vol. 1, no. 1, pp. 38–47, Apr. 2006.

[16] S. Shellhammer, "Spectrum Sensing in IEEE 802.22," in *Proc. of the 1st International Workshop on Cognitive Information Processing (CIP)*, Santorini, Greece, Jun. 2008.